Pure Appl. Geophys. 176 (2019), 3665–3680

https://doi.org/10.1007/s00024-019-02119-1

Pure and Applied Geophysics

# Intraseasonal Convection and Air–Sea Fluxes Over the Indian Monsoon Region Revealed from the Bimodal ISO Index

Gopinadh Konda[1] and Naresh Krishna Vissa[1]

*Abstract*—The present study aims to elucidate the intraseasonal oscillations (ISO) of atmospheric convection and air–sea fluxes over the Indian region during summer monsoon season. To accomplish this, the study employs the extended empirical orthogonal function-based bimodal ISO index developed by Kikuchi et al. [Clim Dyn 38(9–10):1989–2000, 2012]. The propagation of deep convective anomalies and air–sea fluxes are explored during the different phases (P1–P8) of the bimodal index. This is achieved by examining the Tropical Rainfall Measuring Mission satellite rainfall, outgoing long-wave radiation (OLR), sea surface temperatures (SST), downward shortwave radiation (DSR) and reanalysis products of 850-hPa winds, potential vorticity and latent heat fluxes (LHFs). Composite analysis of the anomalies depicts the strong (weak) northward (eastward) propagation of convective anomalies over the Indian region (equatorial Indian Ocean). Over the Indian region, active (suppressed or weak) convection is evident during the phases of P4 and P5 (P1, P2 and P7, P8). Enhanced deep convection is lead by a phase of 850-hPa westerly winds and negative SST anomalies. Signatures of ISO during different phases are examined from Research Moored Array for African-Asian-Australian Monson Analysis and Prediction (RAMA) buoy observations over the Bay of Bengal. Rainfall, SST and LHF anomalies from RAMA buoy measurements are in concurrence with the spatial composites of bimodal ISO phases. Plausible drivers for the variability of intraseasonal convection and air–sea fluxes were reviewed using published observational and modelling studies. Findings from the present study advocate the applicability of Kikuchi bimodal index [Clim Dyn 38(9–10):1989–2000, 2012] over the Indian region and have practical application for the validation of ocean-atmospheric coupled models.

**Key words:** Indian summer monsoon, intraseasonal, bimodal, convection and air–sea fluxes.

## 1. Introduction

### 1.1. Tropical Intraseasonal Oscillations (TISO)

The spatial scales of tropical atmospheric circulations range from a few mm (e.g. turbulent process) to 1000 km (e.g. African easterly waves). Similarly, temporal scales of motions range from a few seconds (e.g. turbulent eddies) to decades (e.g. Pacific decadal oscillations). Though spatial and temporal scales of these tropical oscillations are different, they constantly interplay with one another (e.g. Bonell and Bruijnzeel 2005; Krishnamurti et al. 2013; Anandh et al. 2018). In the tropics, the atmosphere shows a dominant mode of variability at an intraseasonal (20–60 days) scale, often called tropical intraseasonal oscillation (TISO). The TISO displays a significant seasonal variation; during boreal winter it is characterized by eastward propagation along the equator, popularly known as the Madden–Julian oscillation (MJO). In contrast, during the boreal summer, the TISO or boreal summer intraseasonal oscillation (BSISO) exhibits eastward, northward, north-eastward and westward complex propagation over the regions of tropical Indian ocean, western Pacific and western North Pacific (e.g. Madden and Julian 1994; Yun et al. 2010; Krishnamurti et al. 2013; Kikuchi et al. 2012; Lee et al. 2013; Singh and Dasgupta 2017).

The MJO is the best example of the large-scale atmospheric circulations in the tropics; it has characteristic periods of 30–90 days, associated with the deep convection, and propagates eastward at an average speed of 5 m $s^{-1}$ across the equatorial Indian Ocean to the western/central Pacific Ocean. The onset, active and break phases of the summer and winter monsoons are associated with the active and

[1] Department of Earth and Atmospheric Sciences, National Institute of Technology Rourkela, Dist.: Sundargarh, Rourkela, Odisha 769008, India. E-mail: vissan@nitrkl.ac.in; vissanaresh@gmail.com

suppressed convection phases of the MJO over the Indian and Pacific Oceans (e.g. Madden and Julian 1971, 1972; Moncrieff et al. 2012; Zhang 2005; Zhang et al. 2013; Zhu et al. 2017; Anandh et al. 2018). The BSISO has been conceptualized to differentiate it from the MJO (e.g. Lawrence and Webster 2002; Lee et al. 2013; Wang et al. 2018). The main convective zones of the BSISO propagate away from the equator to northern latitudes ($\sim$ 10°N to 20°N) over the Indian sub-continent and western North Pacific (e.g. Yun et al. 2010). In the global monsoon system, the BSISO is one of the most dominant sources of short-term variability of the Asian summer monsoon and the East Asian summer monsoon season (Kikuchi et al. 2012; Lee et al. 2013).

Emanuel (1987) made the first attempt to study the intraseasonal oscillations (ISO) using an air–sea interaction model. His findings suggest that anomalous surface heat fluxes attributed to the temperature perturbations may lead to eastward propagation of 30–60 oscillations. An idealized model has been used to understand the origin of TISO. Eastward propagation of a convective system (clouds) arises in relation with the interaction between the convection and dynamics of the system, and the theory is referred to as the mobile wave conditional instability of second kind (CISK) mechanism. East–west sea surface temperature (SST) distribution can induce changes in the amplitude of the CISK mechanism (Lau and Peng 1987). The TISO dynamics and the roles of convective interaction with tropical boundary layer dynamics such as moisture convergence were examined by Wang and Li (1994). The convergence at the equator plays an important role during the life cycle of the MJO (Maloney and Hartmann 1998). Raymond and Fuchs (2009) hypothesized that the MJO is mainly driven by moisture mode instability. Later, Sobel et al. (2008, 2009) suggested that the heat fluxes from the ocean to atmosphere play a major role in driving the TISO. In the tropical atmosphere, several multiscale processes generate the TISO; these are significantly associated with the organized synoptic-scale circulations (e.g. Majda and Biello 2004). Theories that are responsible for the genesis of TISO were reviewed by Seo and Song (2012). Observational and recent modelling studies indicating that ocean–atmosphere coupling is vital for the sustainability of TISO (e.g. Hu et al. 2017).

Previous observational and modelling studies indicate that the bimodal characteristics of ISO play a vital role during the Indian summer monsoon (ISM) (e.g. Kikuchi et al. 2012). Thus, the spatial and temporal changes of air–sea fluxes and atmospheric convection in relation with the bimodal nature of ISO may enable better understanding of monsoon dynamics. The next section will provide a succinct overview of selected literature of relevance to the work. This will include selected global work and findings from previous contributions undertaken at the much larger Indian continental and South Asian scales.

### *1.2. An Overview of Intraseasonal SST and Air–Sea Flux Variability*

Observations of the TISO have been reviewed by many researchers (e.g. Krishnamurti et al. 1988; Madden and Julian 1994; Zhang 1996; Lau and Sui 1997; Hendon and Glick 1997; Sengupta et al. 2001; Araligidad and Maloney 2008; Zeng and Wang 2009; Kikuchi et al. 2012; Roxy et al. 2013; Wang et al. 2018; Hazra and Krishnamurthy 2018). SST variations can occur at various spatial and temporal scales. Previous researchers have documented well the relationship between the TISO and SST ISO using in situ and satellite measurements. Intraseasonal SST variations and their relation to latent heat fluxes (LHFs) are established using Tropical Ocean Global Atmosphere Tropical Atmosphere–Ocean (TOGA-TAO) moored buoy observations over the equatorial western Pacific Ocean (Zhang and McPhaden 1995). Zhang (1996) used TOGA-TAO observations to examine the surface atmospheric intraseasonal oscillations, and they explained the relationship between the SST and deep convection. In addition, the occurrence of variations at the air–sea interface can play an active role in TISO above the boundary layer. The genesis of the MJO, SST coupling, atmospheric convection and surface fluxes is one of the complex multiscale phenomena (Lau and Sui 1997). Internal dynamics of the MJO produce time-varying SST, which might also affect the evolution of convection. During MJO propagation, the occurrence of maximum SST is reported between the cloudy and fair-

weather regions (Shinoda et al. 1998). Over the western Pacific, intraseasonal variations of SSTs are driven by shortwave radiation and LHFs. In contrast, over the Indian Ocean, SST variations are mainly controlled by shortwave radiation (Shinoda et al. 1998). Jones et al. (1998) revealed the possible feedback mechanism between the MJO and SST variations over the equatorial Pacific and Indian Oceans. The spatial and temporal features of SST and surface heat fluxes on intraseasonal scales revealed the importance of appropriate mixed layer depths over the equatorial Indian Ocean and Pacific Ocean (Woolnough et al. 2000).

The sub-seasonal changes of SST, surface winds and atmospheric convection are well related over the Bay of Bengal (BoB) during the ISM (e.g. Sengupta and Ravichandran 2001; Vecchi and Harrison 2002). The northward propagating ISO or BSISO are closely linked with the underlying SST, surface convergence, vorticity, and surface heat fluxes (Sengupta et al. 2001; Fu et al. 2003; Fu and Wang 2004). Zheng et al. (2004) used the coupled general circulation model to understand the role of SST and TISO, and their findings suggest a near-quadrature relationship between the SST and precipitation with TISO. The air–sea flux variability in the ISO time scale can generate the SST perturbations north of the enhanced convection by two different processes; i.e. by cloud-shortwave radiation and wind evaporation (e.g. Hendon 2005). The BSISO has a typical wavelength of nearly 2000 km, and the northward propagation of the ISO is primarily attributed to the asymmetric specific humidity, internal atmospheric dynamics and air–sea interaction (e.g. Jiang et al. 2004). Roxy and Tanimoto (2007) identified the relationship between the northward-propagating positive SST anomalies (SSTAs) and surface air temperatures with northward-propagating precipitation anomalies. In the South China Sea, intraseasonal oscillations of LHFs reveal that, during the ISM, intraseasonal variations of latent-heat fluxes are well related with the wind speed, whereas during winter season, LHFs are well correlated with winds and surface moisture (Zeng and Wang 2009). The National Centers for Environmental Prediction (NCEP) climate forecast system coupled with regional simulations indicate that intraseasonal composites of surface winds, LHFs, downward shortwave radiation (DSR) and SST could provide the mechanism for the northward propagation of TISO. The total surface enthalpy fluxes and its feedbacks with the TISO are one of the plausible factors in providing the energy sources for TISO disturbances (Sobel et al. 2009). The amplitude of the northward-propagating TISO is consistent with the magnitude of air–sea interactions in the Indian Ocean (Achuthavarier and Krishnamurthy 2011). In the western wing of the North Indian Ocean, i.e. in the Arabian Sea, SST intraseasonal variations are mainly attributed to wind stress variations, whereas in the eastern wing, i.e. the BoB, heat flux variations are primarily driving the intraseasonal SST variations (Vialard et al. 2012). Recently, Zhu et al. (2017) studied the impacts of SST feedback on the MJO propagation across the Maritime Continent. Their findings revealed the importance of meridional winds along with the convectional zonal wind analysis in representing the realistic SST conditions.

### *1.3. Overview of Intraseasonal Oscillation: ISM*

The active and break phases of ISM rainfall are associated to primary oscillations of the TISO (e.g. Ramamurthy 1969; Goswami et al. 1984; Hazra and Krishnamurthy 2018; Srinivas et al. 2018). Active and break spells are the building blocks of the ISM, which are mainly modulated by the ISO such as MJO and BSISO (e.g. Abhik et al. 2013). During the ISM, the ISO are associated with northward and southward propagation of the tropical convergence zone (Goswami and Mohan 2001). Earlier studies pertaining to observational evidences and associated mechanisms of ISO are discussed here. A ‘quadrapole’ structure with dominant modes of 30–60-day and 10–20-day variability is observed over the Asian monsoon domain (Annamalai and Slingo 2001). The genesis of low-pressure systems during the ISM in the North Indian Ocean are linked with the ISO (Goswami et al. 2003). Over the ISM core region, intraseasonal variations (active and break events) are assessed from the daily rainfall data (Rajeevan et al. 2010). During the active periods, the positive rainfall anomalies are evident over the entire peninsular India, whereas during the break periods, active convection migrates towards the northeast India and

over the foothills of the Himalayas (Krishnamurthy and Shukla 2007). Rainfall anomalies over the Indian subcontinent are associated with the ISO of oceanic variables in the western coast of the India peninsula and the northern BoB (Xi et al. 2015). The Tropical Rainfall Measuring Mission (TRMM) rainfall estimates evidently revealed the two complex modes of ISO, i.e. 20–60- and 10–20-day modes, the latter showing a complex north-westward-propagating structure (Karmakar et al. 2017; Karmakar and Krishnamurti 2018).

The key mechanism of low-frequency ISO is provided by Krishnan and Venkatesan (1997), in which their analysis suggests that the northward propagation of monsoonal oscillations is mainly driven by strong north–south differential heating. Atmospheric internal dynamics are mainly attributed to the monsoonal ISO (e.g. Goswami et al. 2006). Air–sea interaction processes such as evolution of SST, surface heat flux and convection are essential for the ISO (Sengupta et al. 2001). Vecchi and Harrison (2002) proposed the air–sea oscillator mechanism in the BoB region to delineate active and break phases of the monsoon. The northward propagation of the BSISO is closely related to the active/break cycles of the Asian summer monsoon (e.g. Lawrence and Webster 2002). Joseph et al. (2010) employed the Development of European Multimodal Ensemble system for seasonal to inTERannual prediction (DEMETER) coupled model to assess the predictability of the interannual variability of the ISM. Their findings suggest that very long breaks during the ISM are associated with the MJO variability. Abhik et al. (2013) proposed a new mechanism for northward propagation of the BSISO based on hydrometeor variability of the upper and lower atmosphere. Air–sea interactions on a sub-daily scale play a significant role in manifesting zonal SST variations; incorporation of sub-daily air–sea interactions may improve the prediction of the ISO over the tropical Asian monsoon region (Hu et al. 2015). The moisture transport from the oceanic and terrestrial sources plays an important role in the zonal and meridional dipoles of rainfall anomalies over the Indian region (Pathak et al. 2017). The warm intraseasonal SSTAs and the associated positive central Indian Ocean mode provide a favourable environment for monsoon ISO (Zhou et al. 2017). During the break periods of the ISM, barotropic instability plays a dominant role, which is evident with a reduction of the distance between the upper-level subtropical westerlies and tropical easterlies (Govardhan et al. 2017). Recent findings suggest that northward propagation of the MJO might contribute to the early, or delay of, monsoon onset over Kerala (e.g. Bhatla et al. 2017). During the drought and flood years of the ISM, the ISO shows distinct characteristics over the BoB and Arabian Sea (Singh and Dasgupta 2017). Recent modelling efforts have been made for better understanding of the ISO during the ISM season using high-resolution regional models (Sperber and Annamalai 2008; Raju et al. 2015; Parekh et al. 2017; Wu et al. 2018). From the above studies, it is clear that during the boreal summer over the Indian region and over the surrounding seas, the ISO shows a distinct bimodal character. In this context, Kikuchi et al. (2012) developed the bimodal ISO index to delineate the active and suppressed periods. Moreover, the bimodal ISO index is useful in defining the phase and amplitude of ISO activity over the tropics across the seasons. The primary focus of the present study is to understand the variability of convection and its relation with air–sea fluxes and potential vorticity anomalies over the Indian region during the ISM (JJAS months) by employing the Kikuchi bimodal ISO index.

## 2. *Data and Methods*

In the recent years, the BoB marine observations have been improved significantly. The efforts from the international oceanography community is highly appreciable through the Indian Ocean Observing System (IndOOS). The Research Moored Array for African-Asian-Australian Monson Analysis and Prediction (RAMA) is an important component of the IndOOS network-based in situ system (McPhaden et al. 2009; Vissa et al. 2013). The parameters included in the present study are SST, precipitation and LHFs (derived) at the six buoys located at the 0°, 1.5°N, 4°N, 8°N, 12°N and 15°N along the 90°E longitude for the period 2008–2015. Turbulent fluxes were computed with the Coupled Ocean–Atmosphere

Response Experiment (COARE) version 3.0 flux algorithm (Fairall et al. 2003) using daily averaged data. The ISO of the rainfall are examined using the daily TRMM 3B42 rain rates for the period 2002–2015 during the ISM season (JJAS), and the study area covers the geographic boundaries 40°E–140°E and 20°S–40°N. Gridded (0.25° × 0.25°) daily SST and 850-hPa winds and potential vorticity are taken from the European Centre for Medium-Range Weather Forecasts (ECMWF) ERA-Interim reanalysis (Gibson et al. 1997). The U.S. NCEP National Center for Atmospheric Research (NCAR) Reanalysis 1 project is using a state-of-the-art analysis/forecast system to perform data assimilation using past data from 1948 to the present (Kalnay et al. 1996). Daily OLR and surface solar radiation downward (SSD) are taken from the NCEP/NCAR available at 2.5° × 2.5° and 2° × 2,° respectively. National Aeronautics and Space Administration released the Modern Era Retrospective-Analysis for Research and Analysis (MERRA) reanalysis dataset in 2010 based on the Goddard Earth Observing System Data Analysis System, version 5 [GEOS-5 DAS; Rienecker et al. (2011)]. This global reanalysis covers the period 1979–present. MERRA takes advantage of a variety of recent satellite data streams. In the present study we use MERRA latent heat flux data for the same period as precipitation, and the spatial resolution of the data is 0.6° × 0.5° (longitude by latitude).

Kikuchi et al. (2012) developed a bimodal ISO index using daily anomalies of outgoing long-wave radiation (OLR), and 850- and 200-hPa zonal winds based on extended empirical orthogonal functions (EEOFs). The first two principal components of the EEOF have been used to derive the amplitude and phase of the bimodal ISO index. The bimodal index-normalized amplitude greater than 1 was considered in the present study (e.g. Yamaura and Kajikawa 2017). The bimodal ISO index used here is available online at http://iprc.soest.hawaii.edu/users/kazuyosh/Bimodal_ISO.html. The composite anomaly of the each variable is extracted for bimodal ISO index phases (P1–P8) by subtracting the JJAS means for the period 2002–2015.

## 3. Results and Discussion

### 3.1. Variability of the Bimodal ISO Index

The bimodal ISO index with amplitude greater than one (active days) are considered for the period 2002–2015 during the JJAS months. The total number of active days during the JJAS months of different years is shown in the Fig. 1. During the years 2002–2008, the numbers of active days are high, whereas in the years 2009–2015, the numbers of active days are decreased. The differences in active days during the two periods can be linked with the northward-propagating acceleration of the BSISO and decrease of convection over the tropical Indian Ocean and the western tropical Pacific (Yamaura and Kajikawa 2017). During 2002 and 2009, the North Indian Ocean and Indian subcontinent experienced severe drought conditions (e.g. Gadgil et al. 2004; Francis and Gadgil 2009). However, during these years, active bimodal ISO days are relatively high (79 and 82 days), active ISO days are associated with inactive convective centres of the Indian Ocean (P1–P3 and P7–P8; not shown here). The average numbers of active bimodal ISO days during the ISM months are shown in Fig. 2; the higher number of active days are noticed during the months of June to August. This signifies the BSISO mode is dominant during the months of June to August; results are in agreement with the Kikuchi et al. (2012) and Li et al. (2016).

### 3.2. Spatial Composite Anomalies of SST, Winds, LHF, OLR, Precipitation and PVA During the Bimodal ISO Phases

Intraseasonal variability of 850-hPa winds is assessed with spatial composites of wind anomalies during the different bimodal ISO index phases (P1 to P8; hereafter, P1 to P8 refers to bimodal ISO index phases), as shown in Fig. 3. Strong intraseasonal variability of 850-hPa wind anomalies is evident during the different phases. During the P2 and P3 phases, easterly wind anomalies are predominant over the North Indian Ocean and Indian peninsula regions, whereas westerly wind anomalies are noticed during P4–P7 bimodal index phases over the ISM core region (50°–95°E, 5°–20°N), and prominently

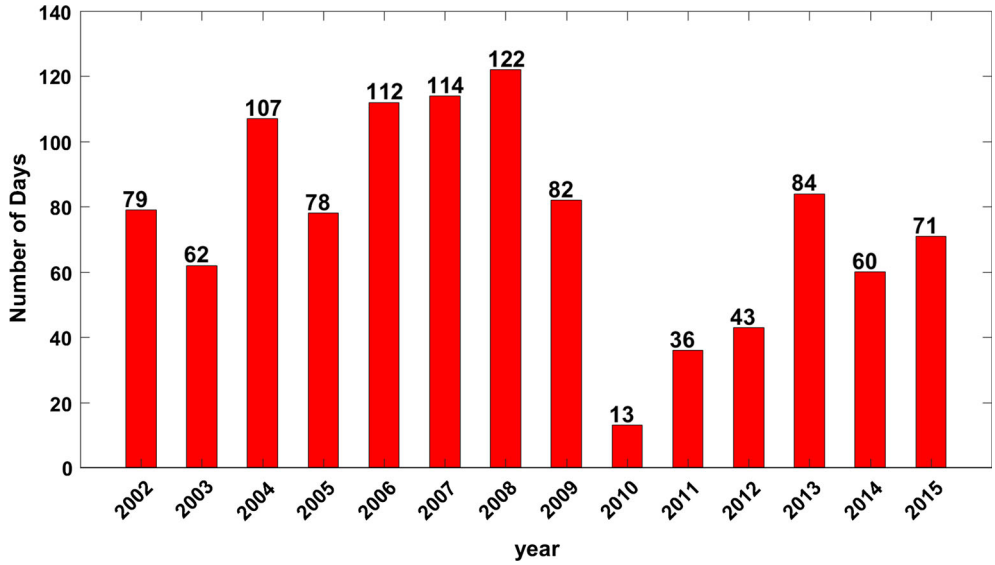


Figure 1
Number of days of the bimodal ISO index (amplitude > 1, for all phases P1 to P8) in each year for the study period 2002 to 2015 during the Indian summer monsoon season (JJAS)

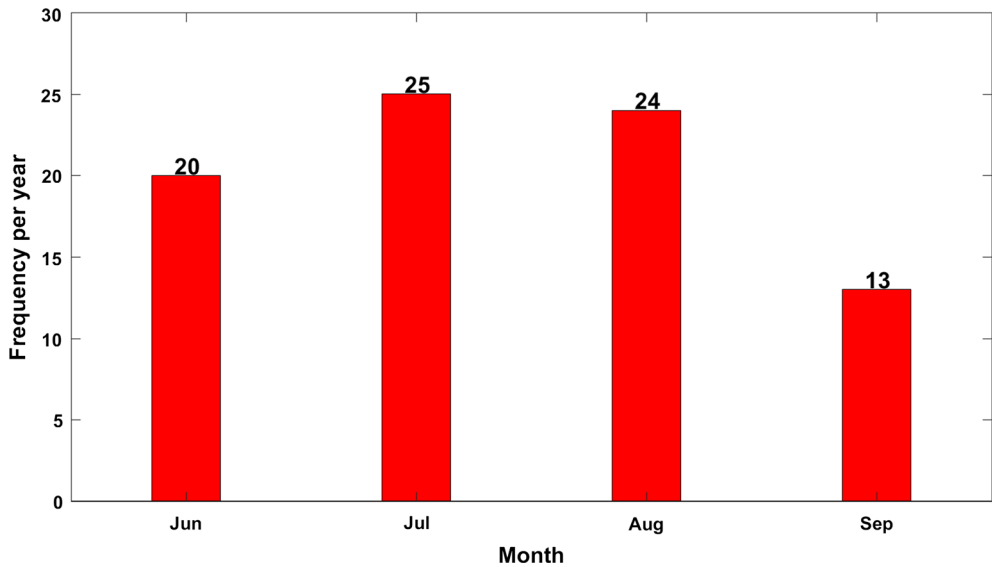


Figure 2
Average number of days per month based on bimodal ISO amplitude

during the P5 and P6 phases. Strengthening of the low-level jet stream around 15–20° north latitudes signifies the active conditions of summer monsoon season (e.g. Webster et al. 2002; Joseph and Sijikumar 2004). Over the equatorial central Indian Ocean (60°E–80°E), westerly (easterly) wind anomalies prevail during the P2 and P3 periods (P5–P7). Spatial composites of SSTAs during the different phases are shown in Fig. 4. During the P6–P8 and P1 phases, negative SSTAs are evident over the Arabian Sea,

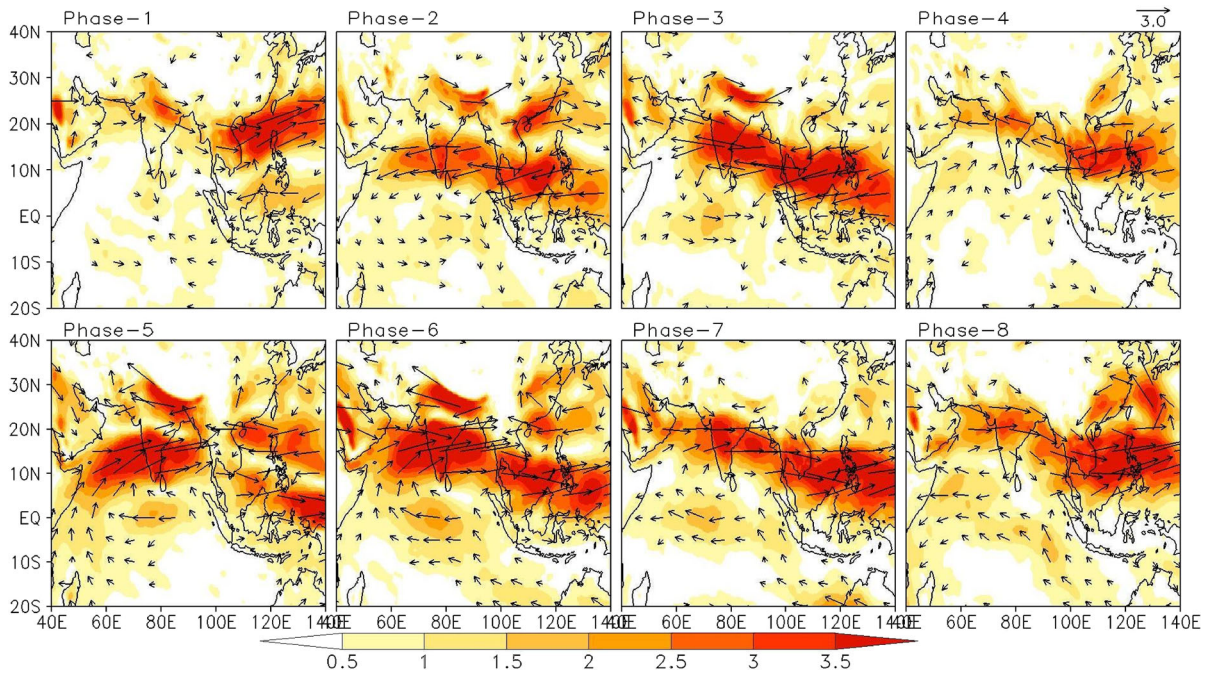


Figure 3
The composite of JJAS 850-hPa wind speed anomalies (m $s^{-1}$) and vectors denotes the direction under different phases (P1 to P8) of the bimodal ISO index for the study period 2002 to 2015

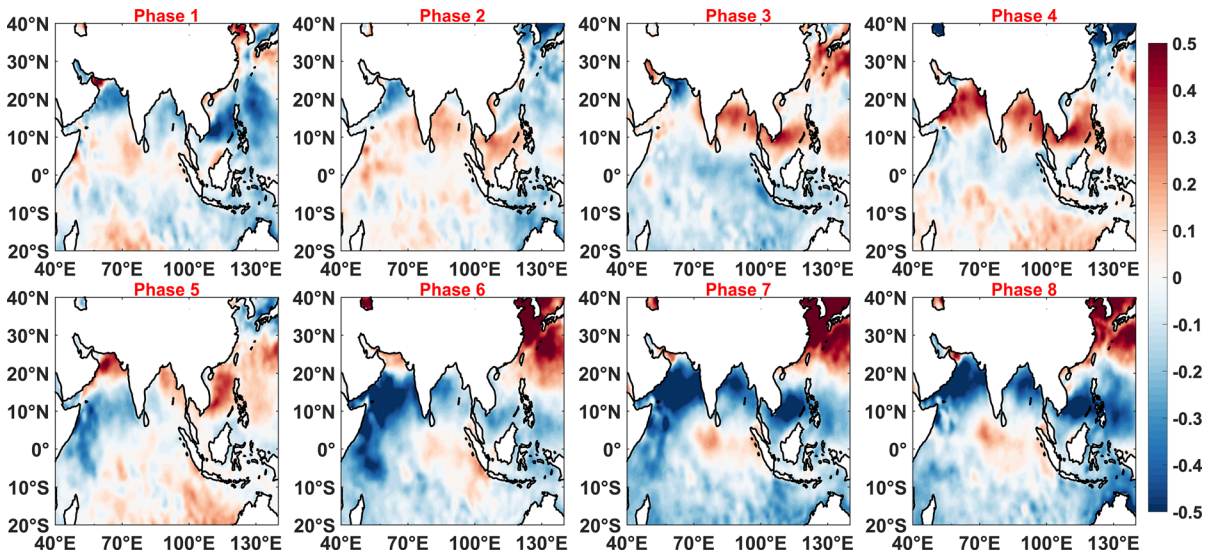


Figure 4
Same as Fig. 3, but for the sea surface temperature anomalies (SSTAs; °C)

BoB and over the South China Sea, whereas positive SSTAs are evident during P2–P5 phases. Initiation of negative SSTAs are evident over the Arabian Sea during phase P5. Negative SSTAs in the south eastern Arabian Sea during phases P4–P6 signify the active monsoon season caused by the propagation of an

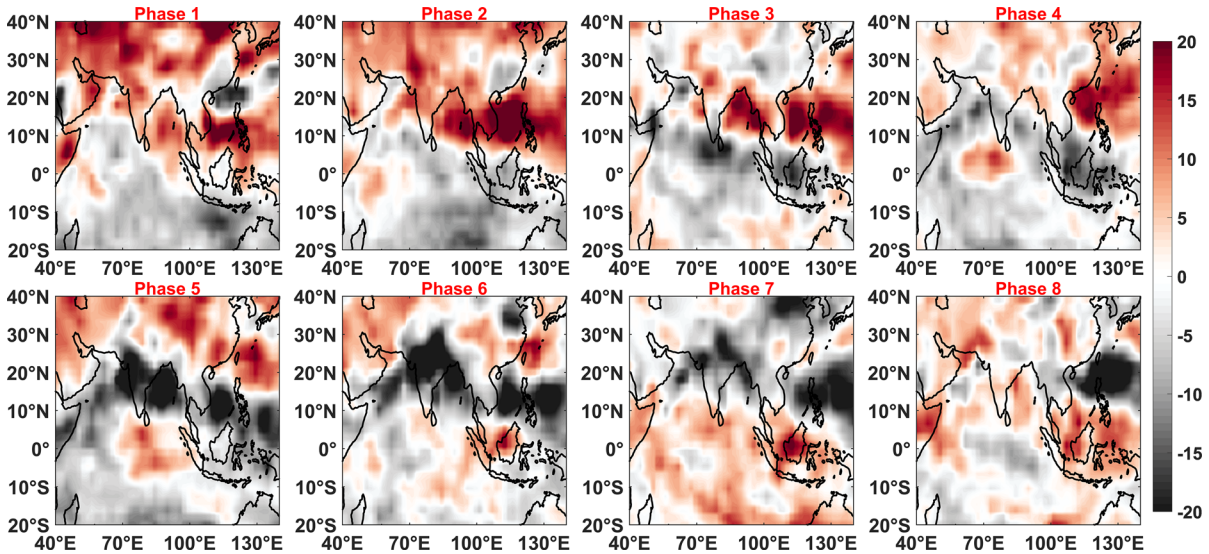


Figure 5
Same as Fig. 3, but for the downward solar radiation anomalies (DSRAs; W $m^{-2}$)

oceanic Rossby wave (Rai et al. 2017). Quasi-mirror images of SSTAs are evident over the equatorial Indian Ocean and North Indian Ocean. Intraseasonal SST variations are mainly attributed to the DSR and LHF (e.g. Hazra and Krishnamurthy 2018). In this context, SSTA perturbations are assessed with the DSR and LHF anomalies (LHFAs) during different phases. This is useful to understand the lead/lag relationship between the SSTA and radiative and turbulent fluxes.

Spatial composites of DSR anomalies (DSRAs) during bimodal index phases (P1 to P8) are shown in Fig. 5. In the north of 10°N, negative (positive) DSRAs are evident during the P4–P7 phases (P1–P3 and P8 phases), whereas weak positive DSRAs in the equatorial Indian Ocean are evident during phases P4–P7. DSRAs and SSTAs are in phase during all the phases, whereas SSTAs lag behind the DSRAs by a phase. Spatial composites of LHFAs during bimodal index phases (P1 to P8) are shown in Fig. 6. During phase P1, the negative LHFAs are prominent over the northern BoB; during phase P3, these anomalies spread over the whole BoB and Arabian Sea, whereas positive LHFAs are seen during phases P5–P7, predominantly over the BoB during phase P5. Similarly, over the equatorial Indian Ocean, positive (negative) LHFAs are evident during phases P1–P3 (P5–P7). Pronounced positive (negative) LHFAs are evident over the regions of negative (positive) SSTAs and westerly (easterlies) wind anomalies. Previous studies (Shinoda et al. 1998) suggested that intraseasonal SST variations over the Indian Ocean are primarily controlled by insolation, whereas the present study reveals that both radiative (DSRAs) and surface heat fluxes (LHFAs) are important in contributing to the SST variations with a phase lead.

Composite OLR anomalies (OLRAs) during bimodal ISO phases (P1–P8) are shown in Fig. 7. Northward, eastward and north-eastward propagation of (negative OLRA) deep convection is depicted during different phases. Over the North Indian Ocean and Indian subcontinent (central equatorial Indian Ocean), active convection is evident during the P4–P6 phases (P1–P3), whereas suppressed convection is evident during phases P1, P2, P7 and P8 (P4–P8). Negative OLRAs and 850-hPa westerly wind anomalies are in phase during all the phases. During the phase P1, convection (negative OLR) is prominent over the equatorial Indian Ocean; from phase P2 onwards it started propagation in the eastward, northward and weak southward direction. During phase P3, convection reached southern India and the

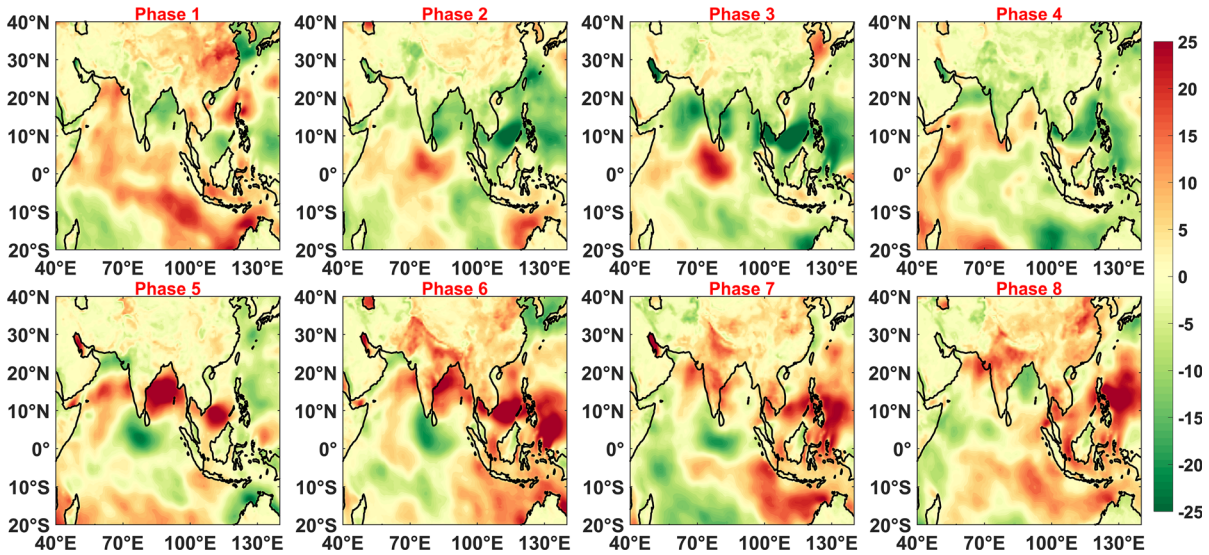


Figure 6
Same as Fig. 3, but for the latent heat flux anomalies (LHFAs; W $m^{-2}$)

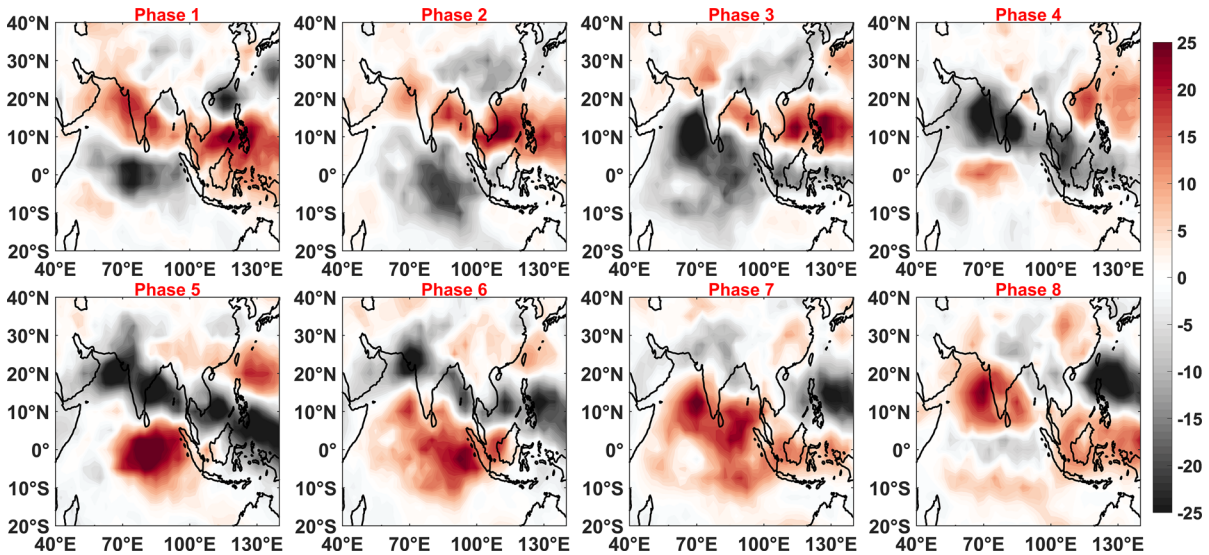


Figure 7
Same as Fig. 3, but for the outgoing long-wave radiation (OLR) anomalies (W $m^{-2}$)

Maritime Continent; in the subsequent phases (P4 and P5), organized convection established over central India and the western Pacific as a tilted band of convection from northwest India to the western Pacific. Similar kinds of intraseasonal variations associated with convection of the eastward-propagating MJO and northward-propagating BSISO are reported by Krishnamurthy (2018) by using multichannel singular spectral analysis. Further, OLRA variations signifying the dipole pattern of positive

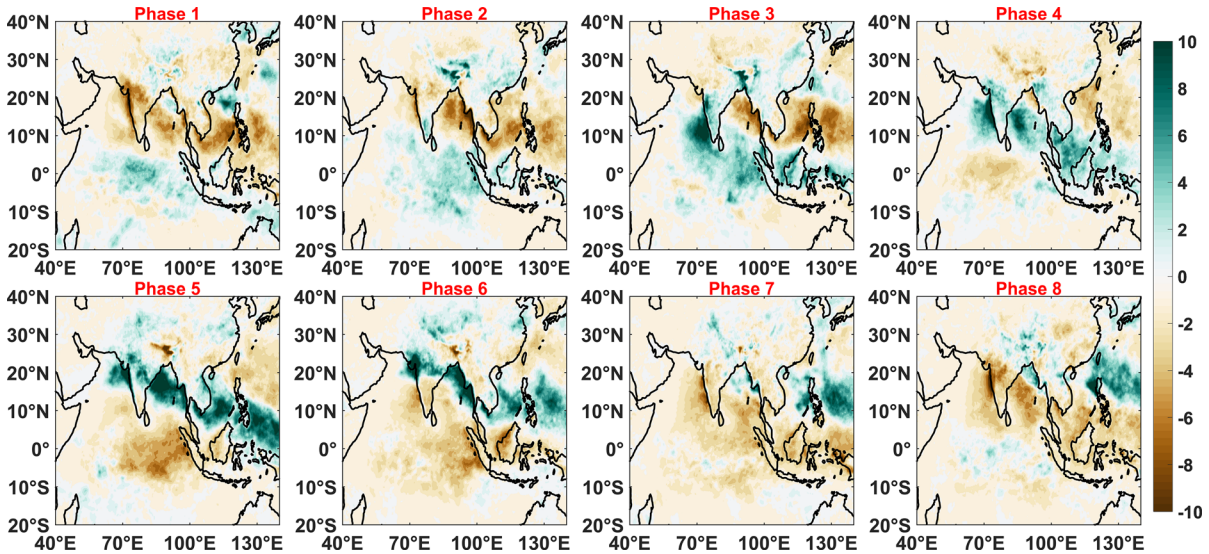


Figure 8
Same as Fig. 3, but for the TRMM 3B42 rainfall anomalies (mm day$^{-1}$)

convective anomalies over the oceanic tropical convergence zone and continental tropical convergence zone during phases P1–P3 and P4–P6, respectively, are in concurrence with the findings of Goswami and Mohan (2001) and Pai et al. (2011). Positive (negative) SSTAs and easterly (westerly) wind anomalies are concurrent in the North Indian Ocean. Deep convection (both eastward and northward) leads the westerly winds by a phase. TRMM rainfall composite anomalies during the different phases are shown in Fig. 8; the rainfall anomalies are in phase and concurrent with the OLR anomalies. Northward (Indian region) and eastward (equatorial Indian Ocean) propagation of positive rainfall anomalies are noticed during phases P4–P6 and P1–P2, respectively. During phase P3, both northward and eastward propagation of active convection is apparent. Negative rainfall anomalies are evident during the phases P1, P2, P7 and P8 over the core Indian summer monsoon region, whereas during phases P2 and P3, positive anomalies are noticed over the leeward side of the Western Ghats (rain-shadow region) and over the eastern side of foothill side of Himalayas (e.g. Tawde and Singh 2015; Anandh et al. 2018). Above normal rainfall over the leeward side of the Western Ghats and foothills of the Himalayas is associated with the break phases of the ISM (e.g. Krishnamurthy and Shukla 2000). Spatial composites of potential vorticity anomalies during different phases are displayed in Fig. 9. The dynamic and thermal state of the atmosphere can be assessed by analysing potential vorticity (e.g. Hoskins and Rodwell 1995; Joseph and Sijikumar 2004; Zhou and Li 2010). The spatial structure of the low-level jet variability at 850 hPa during the active and break phases of the monsoon is elucidated from potential vorticity anomalies (Rai et al. 2017). Intraseasonal potential vorticity anomalies such as significant northward and weak eastward propagation of positive potential vorticity anomalies are evident during the different phases. Potential vorticity anomalies mirror the OLRAs; e.g. over the south (north) of 15°N, positive (negative) potential vorticity anomalies are evident during phases P1–P3 (P4–P7). Negative potential vorticity anomalies over the south-eastern Arabian Sea during phases P5 and P6 could be associated with a decrease of material modification of potential vorticity, which is also evident in the wind patterns; i.e. strong westerly anomalies over southern India. During phases P1–P3, active eastward propagation of convection is evident over the equatorial Indian Ocean; however, low values of potential vorticity

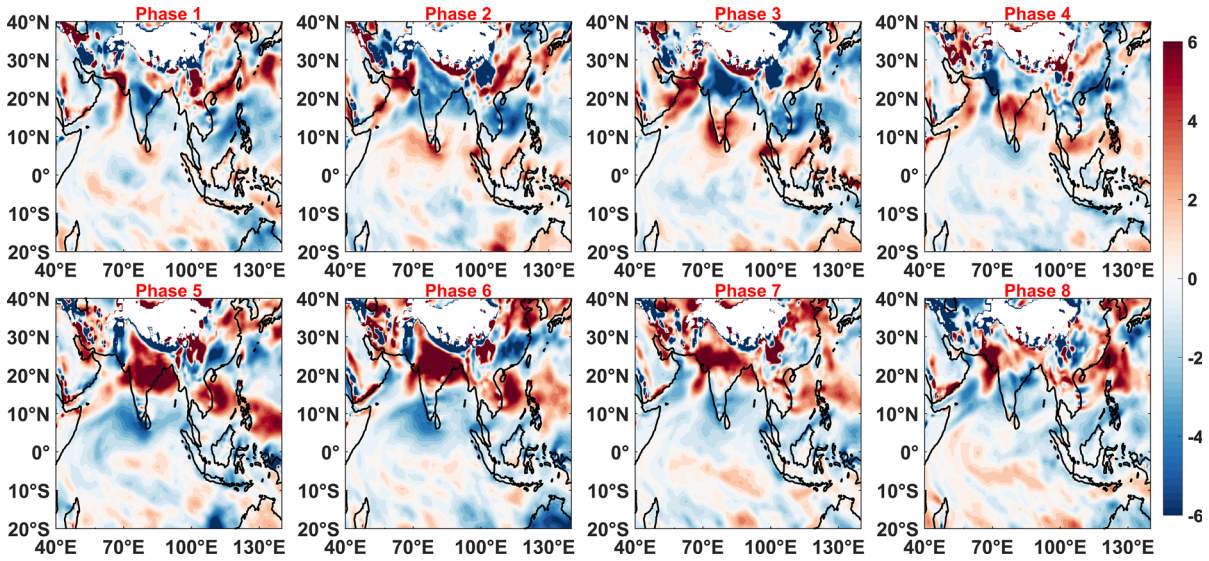


Figure 9
Same as Fig. 3, but for the 850-hPa potential vorticity anomalies ($10^{-8}$ × K $m^2$ $kg^{-1}$ $s^{-1}$)

anomalies are noticed. This could be associated with low values of planetary vorticity ('f') and low relative vorticity values as depicted by the 850-hPa wind anomalies during these phases over equatorial Indian Ocean. Large-scale variability of potential vorticity anomalies during different phases portrayed in the present study is in agreement with the findings of Hoskins and Rodwell (1995), Joseph and Sijikumar (2004) and Rai et al. (2017).

### 3.3. *LHF, Rainfall and SSTA Variability from RAMA Measurements*

During the different phases of the bimodal ISO index, daily composites of latent heat flux, rainfall and SSTAs tracked using six RAMA buoy observations over the BoB along the 90°E at the 0°, 1.5°N, 4°N, 8°N, 12°N and 15°N latitudes are displayed in Fig. 10. In concurrence with the spatial patterns of TRMM rainfall anomalies, positive LHFA and SSTA anomalies at 15°N and 12°N are evident during phases P4 and P5, whereas negative anomalies are noticed during phases P1–P2 and P7–P8. At the lower latitudes (0°, 1.5° and 4°N), variability of anomalies captures the weak eastward propagation of the MJO. A time series of daily LHFA, SSTA and rainfall anomalies at RAMA buoy locations at 15°N and 90°E along with bimodal ISO index phase and amplitude are shown in Fig. 11. For the period 2011–2012, data is missing over the location. Positive (negative) rainfall and LHFAs are evident during the phases P3 to P5 (P1 and P8). Lag between the active convection and negative SSTAs are evident over the location; these results are consistent with Woolnough et al. (2000). Spatial composites are made in the present study with amplitude greater than 1, whereas in this location, observed rainfall anomalies signify that with bimodal ISO and its amplitude $< 1$ also captures the ISO signals.

## 4. *Conclusions*

In the tropics during the ISM, the ISO portrays a bimodal character as an eastward-propagating MJO and a dominant northward-propagating BSISO. The present study examines the intraseasonal atmospheric convection, air–sea fluxes and potential vorticity anomalies during the ISM. Accurate representation of bimodal ISO character is crucial for better understanding of the internal monsoon dynamics and rainfall prediction. In this regard, Kikuchi et al. (2012) developed the bimodal ISO index based on EEOFs. The bimodal ISO index, phases and

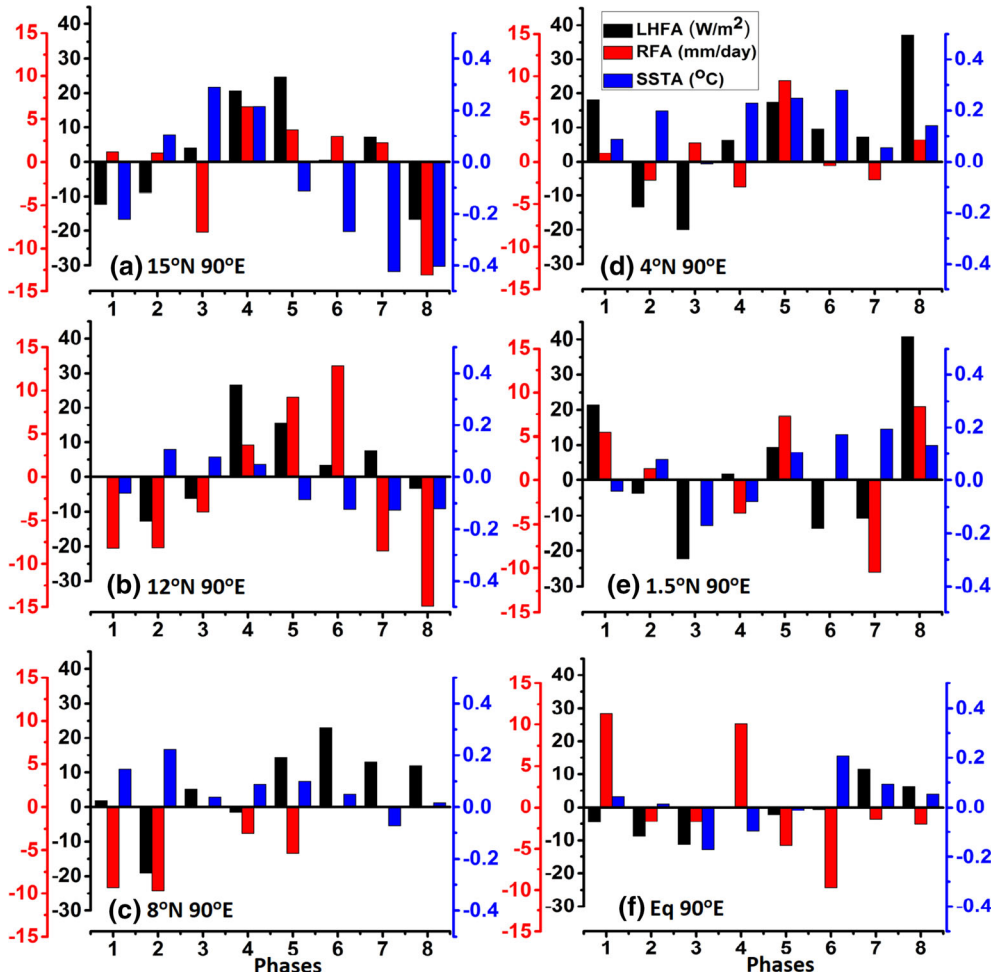


Figure 10
The bimodal ISO index phase composites of latent heat flux (W $m^{-2}$), rainfall (mm $day^{-1}$) and SSTAs (°C) at six RAMA buoy observations along 90°E at the **a** 15°N, **b** 12°N, **c** 8°N, **d** 4°N, **e** 1.5°N and **f** 0°

amplitude specify the location and strength of convective centres of the ISO. In the present study, we have adopted the bimodal ISO index to delineate the representative phases (P1–P8) of northward and eastward propagation of the ISO over the Indian region and surrounding seas. Composite maps of 850-hPa winds, potential vorticity, DSR, LHF, SST, rainfall and OLR anomalies are analysed during the bimodal ISO phases. Active northward (eastward) propagation of the BSISO (MJO) is evident during phases P4–P6 (P1–P2) over the Indian region and North Indian Ocean (central equatorial Indian Ocean), which are associated with negative OLR, DSR and SST, positive LHF, potential vorticity and westerly wind anomalies at 850 hPa. During phase P3, both eastward and northward ISO is evident over the North Indian Ocean. The relationship between the bimodal ISO phases and convective anomaly centres, 850-hPa winds and SSTAs are indicated in Fig. 12. Deep convection (clear sky conditions) leads (by $\sim$ 1 phase) enhanced westerly (easterly) winds and negative (positive) SSTAs; however, this relationship is predominant over the North Indian Ocean. The present study supports the relationship between the ISO convection and surface heat fluxes, documented by Shinoda et al. (1998) and Kemball-Cook and Wang (2001), for the eastward and northward propagation of convective anomalies (the MJO and BSISO),

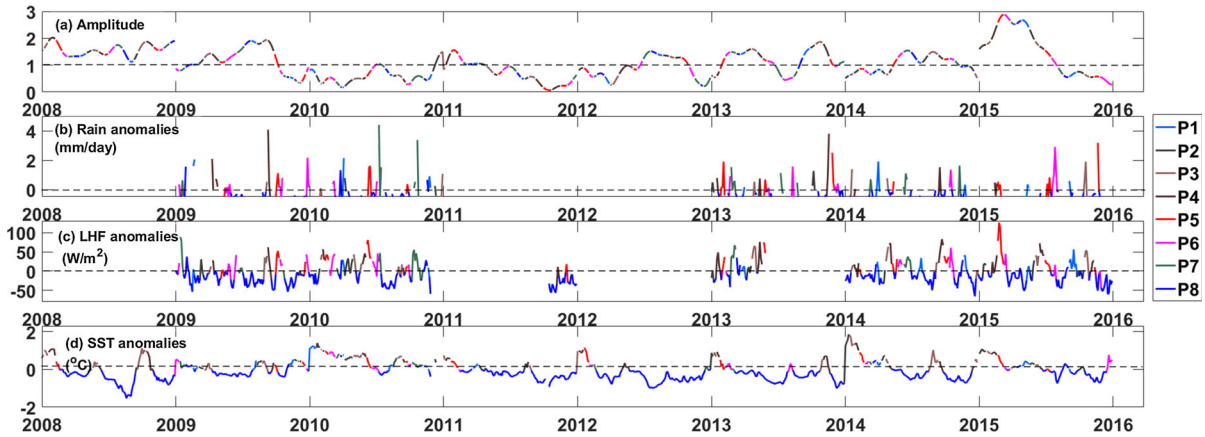


Figure 11
**a** Time series data of bimodal ISO amplitude and phases. RAMA buoy location (15°N, 90°E). **b** Rainfall anomalies (mm day$^{-1}$); **c** LHFAs (W m$^{-2}$); and **d** SSTAs (°C)

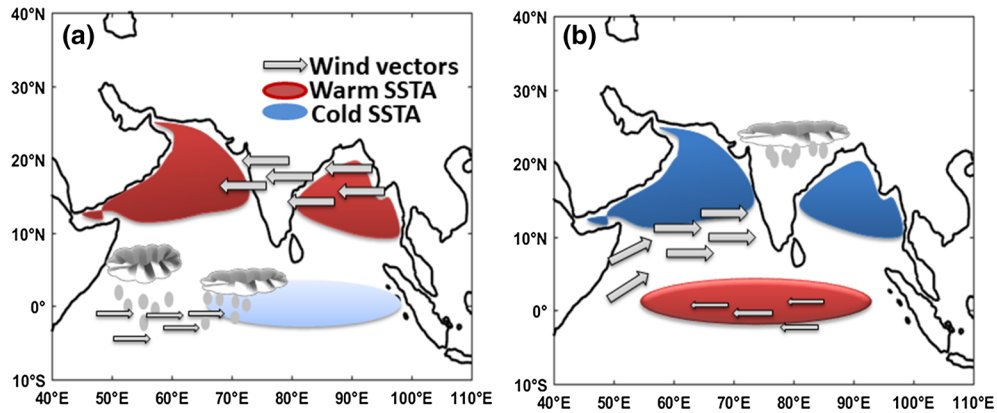


Figure 12
**a** Schematic representation of an active eastward propagation of the MJO during phases P1 and P2; **b** an active northward propagation of the BSISO during phases P4 and P5

respectively, for the summer monsoon season. Kikuchi et al. (2012) were able to delineate and represent the bimodal character of the ISO in terms of air–sea fluxes and convection over the Indian Ocean. The present study advocates that the bimodal ISO index has practical application to ocean-atmospheric coupled models during the summer monsoon season.

## *Acknowledgements*

The authors would like to acknowledge the Department of Science and Technology, Government of India [Science and Engineering Research Board (grant ref: ECR/2016/001896)]. NKV would like to thank late Prof. M. Bonell (University of Dundee, UK) for sharing his wonderful knowledge and experience on this topic. The authors would like to thank the editors Dr. M Ravichandran and Dr. VSN Murty for their initial comments. The authors are grateful to the anonymous reviewers for their meticulous comments and valuable suggestions.

## References


Abhik, S., Halder, M., Mukhopadhyay, P., Jiang, X., & Goswami, B. N. (2013). A possible new mechanism for northward propagation of boreal summer intraseasonal oscillations based on TRMM and MERRA reanalysis. *Climate Dynamics, 40*(7–8), 1611–1624.

Achuthavarier, D., & Krishnamurthy, V. (2011). Role of Indian and Pacific SST in Indian summer monsoon intraseasonal variability. *Journal of Climate, 24*(12), 2915–2930.

Anandh, P. C., Vissa, N. K., & Broderick, C. (2018). Role of MJO in modulating rainfall characteristics observed over India in all seasons utilizing TRMM. *International Journal of Climatology, 38*(5), 2352–2373.

Annamalai, H., & Slingo, J. M. (2001). Active/break cycles: Diagnosis of the intraseasonal variability of the Asian summer monsoon. *Climate Dynamics, 18*(1–2), 85–102.

Araligidad, N. M., & Maloney, E. D. (2008). Wind-driven latent heat flux and the intraseasonal oscillation. *Geophysical Research Letters*. https://doi.org/10.1029/2007GL032746.

Bhatla, R., Singh, M., & Pattanaik, D. R. (2017). Impact of Madden-Julian oscillation on onset of summer monsoon over India. *Theoretical and Applied Climatology, 128*(1–2), 381–391.

Bonell, M., & Bruijnzeel, L. A. (Eds.). (2005). *Forests, water and people in the humid tropics: Past, present and future hydrological research for integrated land and water management*. Cambridge: Cambridge University Press.

Emanuel, K. A. (1987). An air–sea interaction model of intraseasonal oscillations in the tropics. *Journal of the atmospheric sciences, 44*(16), 2324–2340.

Fairall, C. W., Bradley, E. F., Hare, J. E., Grachev, A. A., & Edson, J. B. (2003). Bulk parameterization of air–sea fluxes: Updates and verification for the COARE algorithm. *Journal of Climate, 16*(4), 571–591.

Francis, P. A., & Gadgil, S. (2009). The aberrant behaviour of the Indian monsoon in June 2009. *Current Science, 97*(9), 1291–1295.

Fu, X., & Wang, B. (2004). The boreal-summer intraseasonal oscillations simulated in a hybrid coupled atmosphere-ocean model. *Monthly Weather Review, 132*(11), 2628–2649.

Fu, X., Wang, B., Li, T., & McCreary, J. P. (2003). Coupling between northward-propagating, intraseasonal oscillations and sea surface temperature in the Indian Ocean. *Journal of the Atmospheric Sciences, 60*(15), 1733–1753.

Gadgil, S., Vinayachandran, P. N., Francis, P. A., & Gadgil, S. (2004). Extremes of the Indian summer monsoon rainfall, ENSO and equatorial Indian Ocean oscillation. *Geophysical Research Letters*. https://doi.org/10.1029/2004GL019733.

Gibson, J. K., Kallberg, P., Uppala, S., Hernandez, A., Nomura, A., & Serrano, E. (1997). ERA description. ECMWF Re-Analysis Project Report Series 1, ECMWF. Reading, United Kingdom, p. 77.

Goswami, B. N., Ajayamohan, R. S., Xavier, P. K., & Sengupta, D. (2003). Clustering of synoptic activity by Indian summer monsoon intraseasonal oscillations. *Geophysical Research Letters*. https://doi.org/10.1029/2002GL016734.

Goswami, B. N., & Mohan, R. A. (2001). Intraseasonal oscillations and interannual variability of the Indian summer monsoon. *Journal of Climate, 14*(6), 1180–1198.

Goswami, B. N., Shukla, J., Schneider, E. K., & Sud, Y. C. (1984). Study of the dynamics of the intertropical convergence zone with a symmetric version of the GLAS climate model. *Journal of the atmospheric sciences, 41*(1), 5–19.

Goswami, B. N., Wu, G., & Yasunari, T. (2006). The annual cycle, intraseasonal oscillations, and roadblock to seasonal predictability of the Asian summer monsoon. *Journal of Climate, 19*(20), 5078–5099.

Govardhan, D., Rao, V. B., & Ashok, K. (2017). Understanding the revival of the Indian summer monsoon after breaks. *Journal of the Atmospheric Sciences, 74*(5), 1417–1429.

Hazra, A., & Krishnamurthy, V. (2018). Seasonality and mechanisms of tropical intraseasonal oscillations. *Climate Dynamics, 50*(1–2), 179–199.

Hendon, H. H. (2005). Air sea interaction. In W. K. M. Lau & D. E. Waliser (Eds.), *Intraseasonal variability in the atmosphere-ocean climate system* (p. 436). Chichester: Praxis Publishing.

Hendon, H. H., & Glick, J. (1997). Intraseasonal air–sea interaction in the tropical Indian and Pacific Oceans. *Journal of Climate, 10*(4), 647–661.

Hoskins, B. J., & Rodwell, M. J. (1995). A model of the Asian summer monsoon. Part I: The global scale. *Journal of the Atmospheric Sciences, 52*(9), 1329–1340.

Hu, W., Duan, A., & He, B. (2017). Evaluation of intra-seasonal oscillation simulations in IPCC AR5 coupled GCMs associated with the Asian summer monsoon. *International Journal of Climatology, 37,* 476–496.

Hu, W., Duan, A., & Wu, G. (2015). Impact of subdaily air–sea interaction on simulating intraseasonal oscillations over the tropical Asian monsoon region. *Journal of Climate, 28*(3), 1057–1073.

Jiang, X., Li, T., & Wang, B. (2004). Structures and mechanisms of the northward propagating boreal summer intraseasonal oscillation. *Journal of Climate, 17*(5), 1022–1039.

Jones, C., Waliser, D. E., & Gautier, C. (1998). The influence of the Madden–Julian oscillation on ocean surface heat fluxes and sea surface temperature. *Journal of Climate, 11*(5), 1057–1072.

Joseph, P. V., & Sijikumar, S. (2004). Intraseasonal variability of the low-level jet stream of the Asian summer monsoon. *Journal of Climate, 17*(7), 1449–1458.

Joseph, S., Sahai, A. K., & Goswami, B. N. (2010). Boreal summer intraseasonal oscillations and seasonal Indian monsoon prediction in DEMETER coupled models. *Climate Dynamics, 35*(4), 651–667.

Kalnay, E., Kanamitsu, M., Kistler, R., Collins, W., Deaven, D., Gandin, L., et al. (1996). The NCEP/NCAR 40-year reanalysis project. *Bulletin of the American Meteorological Society, 77*(3), 437–471.

Karmakar, N., Chakraborty, A., & Nanjundiah, R. S. (2017). Space-Time Evolution of the Low-and High-Frequency Intraseasonal Modes of the Indian Summer Monsoon. *Monthly Weather Review, 145*(2), 413–435.

Karmakar, N., & Krishnamurti, T. N. (2018). Characteristics of northward propagating intraseasonal oscillation in the Indian summer monsoon. *Climate Dynamics*. https://doi.org/10.1007/s00382-018-4268-2.

Kemball-Cook, S., & Wang, B. (2001). Equatorial waves and air–sea interaction in the boreal summer intraseasonal oscillation. *Journal of Climate, 14*(13), 2923–2942.

Kikuchi, K., Wang, B., & Kajikawa, Y. (2012). Bimodal representation of the tropical intraseasonal oscillation. *Climate Dynamics, 38*(9–10), 1989–2000.

Krishnamurthy, V. (2018). Intraseasonal oscillations in East Asian and South Asian monsoons. *Climate Dynamics, 51*(11–12), 4185–4205.

Krishnamurthy, V., & Shukla, J. (2000). Intraseasonal and interannual variability of rainfall over India. *Journal of Climate, 13*(24), 4366–4377.

Krishnamurthy, V., & Shukla, J. (2007). Intraseasonal and seasonally persisting patterns of Indian monsoon rainfall. *Journal of Climate, 20*(1), 3–20.

Krishnamurti, T. N., Oosterhof, D. K., & Mehta, A. V. (1988). Air–sea interaction on the time scale of 30 to 50 days. *Journal of the atmospheric sciences, 45*(8), 1304–1322.

Krishnamurti, T. N., Stefanova, L., & Misra, V. (2013). Scale interactions. In: *Tropical meteorology* (pp. 169–196). Springer, New York, NY.

Krishnan, R., & Venkatesan, C. (1997). Mechanisms of low frequency intraseasonal oscillations of the Indian summer monsoon. *Meteorology and Atmospheric Physics, 62*(1–2), 101–128.

Lau, K. M., & Peng, L. (1987). Origin of low-frequency (intraseasonal) oscillations in the tropical atmosphere. Part I: basic theory. *Journal of the Atmospheric Sciences, 44*(6), 950–972.

Lau, K. M., & Sui, C. H. (1997). Mechanisms of short-term sea surface temperature regulation: Observations during TOGA COARE. *Journal of Climate, 10*(3), 465–472.

Lawrence, D. M., & Webster, P. J. (2002). The boreal summer intraseasonal oscillation: Relationship between northward and eastward movement of convection. *Journal of the atmospheric sciences, 59*(9), 1593–1606.

Lee, J. Y., Wang, B., Wheeler, M. C., Fu, X., Waliser, D. E., & Kang, I. S. (2013). Real-time multivariate indices for the boreal summer intraseasonal oscillation over the Asian summer monsoon region. *Climate Dynamics, 40*(1–2), 493–509.

Li, K., Li, Z., Yang, Y., Xiang, B., Liu, Y., & Yu, W. (2016). Strong modulations on the Bay of Bengal monsoon onset vortex by the first northward-propagating intra-seasonal oscillation. *Climate Dynamics, 47*(1–2), 107–115.

Madden, R. A., & Julian, P. R. (1971). Detection of a 40–50 day oscillation in the zonal wind in the tropical Pacific. *Journal of the atmospheric sciences, 28*(5), 702–708.

Madden, R. A., & Julian, P. R. (1972). Description of global-scale circulation cells in the tropics with a 40–50 day period. *Journal of the atmospheric sciences, 29*(6), 1109–1123.

Madden, R. A., & Julian, P. R. (1994). Observations of the 40–50-day tropical oscillation—a review. *Monthly Weather Review, 122*(5), 814–837.

Majda, A. J., & Biello, J. A. (2004). A multiscale model for tropical intraseasonal oscillations. *Proceedings of the National academy of Sciences of the United States of America, 101*(14), 4736–4741.

Maloney, E. D., & Hartmann, D. L. (1998). Frictional moisture convergence in a composite life cycle of the Madden–Julian oscillation. *Journal of Climate, 11*(9), 2387–2403.

McPhaden, M. J., Meyers, G., Ando, K., Masumoto, Y., Murty, V. S. N., Ravichandran, M., et al. (2009). RAMA: the research moored array for African–Asian–Australian monsoon analysis and prediction. *Bulletin of the American Meteorological Society, 90*(4), 459–480.

Moncrieff, M. W., Waliser, D. E., Miller, M. J., Shapiro, M. A., Asrar, G. R., & Caughey, J. (2012). Multiscale convective organization and the YOTC virtual global field campaign. *Bulletin of the American Meteorological Society, 93*(8), 1171–1187.

Pai, D. S., Bhate, J., Sreejith, O. P., & Hatwar, H. R. (2011). Impact of MJO on the intraseasonal variation of summer monsoon rainfall over India. *Climate Dynamics, 36*(1–2):41–55.

Parekh, A., Raju, A., Chowdary, J. S., & Gnanaseelan, C. (2017). Impact of satellite data assimilation on the predictability of monsoon intraseasonal oscillations in a regional model. *Remote Sensing Letters, 8*(7), 686–695.

Pathak, A., Ghosh, S., Kumar, P., & Murtugudde, R. (2017). Role of oceanic and terrestrial atmospheric moisture sources in intraseasonal variability of Indian summer monsoon rainfall. *Scientific reports, 7*(1), 12729.

Rai, P., Joshi, M., Dimri, A. P., & Turner, A. G. (2017). The role of potential vorticity anomalies in the Somali Jet on Indian Summer Monsoon Intraseasonal Variability. *Climate Dynamics, 50,* 1–21.

Rajeevan, M., Gadgil, S., & Bhate, J. (2010). Active and break spells of the Indian summer monsoon. *Journal of Earth System Science, 119*(3), 229–247.

Raju, A., Parekh, A., Chowdary, J. S., & Gnanaseelan, C. (2015). Assessment of the Indian summer monsoon in the WRF regional climate model. *Climate Dynamics, 44*(11–12), 3077–3100.

Ramamurthy, K. (1969). Some aspects of the 'Break'in the Indian southwest monsoon during July and August FMU Rep. No. IV-1813, January.

Raymond, D. J., & Fuchs, Ž. (2009). Moisture modes and the Madden–Julian oscillation. *Journal of Climate, 22*(11), 3031–3046.

Rienecker, M. M., Suarez, M. J., Gelaro, R., Todling, R., Bacmeister, J., Liu, E., et al. (2011). MERRA: NASA's modern-era retrospective analysis for research and applications. *Journal of Climate, 24*(14), 3624–3648.

Roxy, M., & Tanimoto, Y. (2007). Role of SST over the Indian Ocean in influencing the intraseasonal variability of the Indian summer monsoon. *Journal of the Meteorological Society of Japan Ser II, 85*(3), 349–358.

Roxy, M., Tanimoto, Y., Preethi, B., Terray, P., & Krishnan, R. (2013). Intraseasonal SST-precipitation relationship and its spatial variability over the tropical summer monsoon region. *Climate Dynamics, 41*(1), 45–61.

Sengupta, D., Goswami, B. N., & Senan, R. (2001). Coherent intraseasonal oscillations of ocean and atmosphere during the Asian summer monsoon. *Geophysical Research Letters, 28*(21), 4127–4130.

Sengupta, D., & Ravichandran, M. (2001). Oscillations of Bay of Bengal sea surface temperature during the 1998 summer monsoon. *Geophysical Research Letters, 28*(10), 2033–2036.

Seo, K. H., & Song, E. J. (2012). Initiation of boreal summer intraseasonal oscillation: Dynamic contribution by potential vorticity. *Monthly Weather Review, 140*(6), 1748–1760.

Shinoda, T., Hendon, H. H., & Glick, J. (1998). Intraseasonal variability of surface fluxes and sea surface temperature in the tropical western Pacific and Indian Oceans. *Journal of Climate, 11*(7), 1685–1702.

Singh, C., & Dasgupta, P. (2017). Unraveling the spatio-temporal structure of the atmospheric and oceanic intra-seasonal oscillations during the contrasting monsoon seasons. *Atmospheric Research, 192,* 48–57.

Sobel, A. H., Maloney, E. D., Bellon, G., & Frierson, D. M. (2008). The role of surface heat fluxes in tropical intraseasonal oscillations. *Nature Geoscience, 1*(10), 653.

Sobel, A. H., Maloney, E. D., Bellon, G., & Frierson, D. M. (2009). Surface fluxes and tropical intraseasonal variability: A reassessment. *Journal of Advances in Modeling Earth Systems*. https://doi.org/10.3894/JAMES.2010.2.2.

Sperber, K. R., & Annamalai, H. (2008). Coupled model simulations of boreal summer intraseasonal (30–50 day) variability, Part 1: Systematic errors and caution on use of metrics. *Climate Dynamics, 31*(2–3), 345–372.

Srinivas, G., Chowdary, J. S., Kosaka, Y., Gnanaseelan, C., Parekh, A., & Prasad, K. V. S. R. (2018). Influence of the Pacific-Japan Pattern on Indian Summer Monsoon Rainfall. *Journal of Climate, 31*(10), 3943–3958.

Tawde, S. A., & Singh, C. (2015). Investigation of orographic features influencing spatial distribution of rainfall over the Western Ghats of India using satellite data. *International Journal of Climatology, 35*(9), 2280–2293.

Vecchi, G. A., & Harrison, D. E. (2002). Monsoon breaks and subseasonal sea surface temperature variability in the Bay of Bengal. *Journal of Climate, 15*(12), 1485–1493.

Vialard, J., Jayakumar, A., Gnanaseelan, C., Lengaigne, M., Sengupta, D., & Goswami, B. N. (2012). Processes of 30–90 days sea surface temperature variability in the northern Indian Ocean during boreal summer. *Climate Dynamics, 38*(9–10), 1901–1916.

Vissa, N. K., Satyanarayana, A. N. V., & Kumar, B. P. (2013). Intensity of tropical cyclones during pre-and post-monsoon seasons in relation to accumulated tropical cyclone heat potential over Bay of Bengal. *Natural Hazards, 68*(2), 351–371.

Wang, B., & Li, T. (1994). Convective interaction with boundary-layer dynamics in the development of a tropical intraseasonal system. *Journal of the atmospheric sciences, 51*(11), 1386–1400.

Wang, T., Yang, X. Q., Fang, J., Sun, X., & Ren, X. (2018). Role of air–sea Interaction in the 30–60-Day Boreal Summer Intraseasonal Oscillation over the Western North Pacific. *Journal of Climate, 31*(4), 1653–1680.

Webster, P. J., Clark, C., Cherikova, G., Fasullo, J., Han, W., Loschnigg, J., et al. (2002). The monsoon as a self-regulating coupled ocean—atmosphere system. *International Geophysics, 83,* 198–219.

Woolnough, S. J., Slingo, J. M., & Hoskins, B. J. (2000). The relationship between convection and sea surface temperature on intraseasonal timescales. *Journal of Climate, 13*(12), 2086–2104.

Wu, L., Wong, S., Wang, T., & Huffman, G. J. (2018). Moist convection: a key to tropical wave–moisture interaction in Indian monsoon intraseasonal oscillation. *Climate Dynamics, 51,* 1–12.

Xi, J., Zhou, L., Murtugudde, R., & Jiang, L. (2015). Impacts of intraseasonal SST anomalies on precipitation during Indian summer monsoon. *Journal of Climate, 28*(11), 4561–4575.

Yamaura, T., & Kajikawa, Y. (2017). Decadal change in the boreal summer intraseasonal oscillation. *Climate Dynamics, 48*(9–10), 3003–3014.

Yun, K. S., Seo, K. H., & Ha, K. J. (2010). Interdecadal change in the relationship between ENSO and the intraseasonal oscillation in East Asia. *Journal of Climate, 23*(13), 3599–3612.

Zeng, L., & Wang, D. (2009). Intraseasonal variability of latent-heat flux in the South China Sea. *Theoretical and Applied Climatology, 97*(1–2), 53–64.

Zhang, C. (1996). Atmospheric intraseasonal variability at the surface in the tropical western Pacific Ocean. *Journal of the atmospheric sciences, 53*(5), 739–758.

Zhang, C. (2005). Madden-Julian oscillation. *Reviews of Geophysics, 43,* 2. https://doi.org/10.1029/2004RG000158.

Zhang, C., Gottschalck, J., Maloney, E. D., Moncrieff, M. W., Vitart, F., Waliser, D. E., et al. (2013). Cracking the MJO nut. *Geophysical Research Letters, 40*(6), 1223–1230.

Zhang, G. J., & Mcphaden, M. J. (1995). The relationship between sea surface temperature and latent heat flux in the equatorial Pacific. *Journal of Climate, 8*(3), 589–605.

Zheng, Y., Waliser, D. E., Stern, W. F., & Jones, C. (2004). The role of coupled sea surface temperatures in the simulation of the tropical intraseasonal oscillation. *Journal of Climate, 17*(21), 4109–4134.

Zhou, C., & Li, T. (2010). Upscale feedback of tropical synoptic variability to intraseasonal oscillations through the nonlinear rectification of the surface latent heat flux. *Journal of Climate, 23*(21), 5738–5754.

Zhou, L., Murtugudde, R., Chen, D., & Tang, Y. (2017). Seasonal and interannual variabilities of the central Indian Ocean mode. *Journal of Climate, 30*(16), 6505–6520.

Zhu, J., Wang, W., & Kumar, A. (2017). Simulations of MJO propagation across the Maritime continent: impacts of SST feedback. *Journal of Climate, 30*(5), 1689–1704.

(Received September 25, 2018, revised December 25, 2018, accepted January 28, 2019, Published online February 5, 2019)